**Supporting Information Available:**

# Azo-linked Porous Triptycene Network as absorbents for $CO_2$ and iodine uptake

**Qin-Qin Dang, Xiao-Min Wang, Yu-Fen Zhan, and Xian-Ming Zhang***

†School of Chemistry& Material Science, Shanxi Normal University, Linfen, Shanxi 041004, China
E-mail: zhangxm@dns.sxnu.edu.cn

## Section 1. Materials and Measurements

Triptycene, zinc, and activated carbon (BET=600 $m^2 g^{-1}$) were obtained from Aldrich. Zeolite 13X (pore volume =0.34 $cm^3 g^{-1}$) was obtained from Aladdin Chemical Reagent Factory. Other organic solvents for reactions were distilled over appropriate drying reagents under nitrogen. Deuterated solvents for NMR measurement were obtained from Aldrich.

$^1$H spectra were recorded on a Bruker Advance III 600M NMR spectrometer. The elemental analysis was carried out using Elementar vario MACRO cube Elemental Analyzer. An infrared (IR) spectrum was carried out using KBr pellets on a Variann 640 FT-IR spectrometer. The thermogravimetric analysis (TGA) was performed using a METTLER-TOLEDO thermal analyzer system at the heating rate of 10$^o$C/min in $N_2$ atmosphere. Solid-state NMR experiment was carried on a Varian Infinityplus-400 wide-bore (89 mm) NMR spectrometer at a proton frequency of 399.7 MHz using a 5 mm double-resonance HX CP/MAS NMR probe. $^{13}$C chemical shifts were referenced externally to tetramethylsilane using adamantane as a secondary reference. The $N_2$ isotherm measurements were carried out at 77 K in a liquid nitrogen bath and 273 K in an ice water mixture bath. The $H_2$ sorption isotherms were collected at 77 K in a liquid nitrogen bath and 87 K in a liquid argon bath. The $CO_2$ sorption isotherms were collected at 273 K in an ice water mixture bath and 298 K in an electric heating jacket. The dry samples were loaded into sample tubes and activated under high vacuum (less than 10-5 Torr) at 150 $^o$C. The apparent surface areas were calculated from nitrogen adsorption data by multipoint BET analysis. The apparent micropore distributions were calculated from nitrogen adsorption data by the NLDFT method. The X-ray diffraction (XRD) measurements were performed on a BrukerD8 Advance X-ray diffractometer using CuK α1 irradiation (λ= 0.154 nm). SEM micrographs were performing on JEOL-JSM-6300 under an accelerating voltage of 20-30 kV. UV/Vis spectra have been carried out on a Perkin Elmer Lambda 950 spectrophotometer within the wavelength range 200–700 nm, using the same solvent in the analyzed solution as a blank. X-ray photoelectron spectroscopy (XPS) data were acquired with an ESCA-Lab220i-XL electron spectrometer (VG Scientific Ltd., UK) using 300W Al Kα radiation.

## Section 2. General Synthetic Routes

### Synthesis of Trinitrotriptycene (TNTP)

Trinitrotriptycenes was synthesized according to published methods[S1]. To triptycene (2.5 g, 10 mmol) was added concentrated $HNO_3$ (100 mL) and the mixture was heated at 75 °C for 24 h. The brown solution was cooled to room temperature, then poured into $H_2O$ (1000 mL) and stirred. The precipitate was collected, washed with cooled water, and then dried in air. The crude products were separated by column chromatography on silica gel with dichloromethane/petroleum ether (1:1) as eluent to afford the white solids TNTP. Yield, 64%; $^1H$ NMR (600 MHz, $CDCl_3$): δ 5.82 (s, 1H), 5.84 (s,1H), 7.63-7.66 (m, 3H), 8.04-8.07 (m, 3H), 8.32-8.34 (m, 3H).

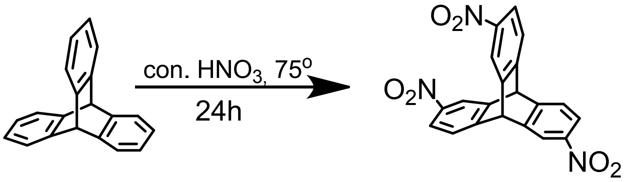

**Scheme S1.** Reaction for the synthesis of trinitrotriptycenes.

## Section 3. IR and NMR spectra

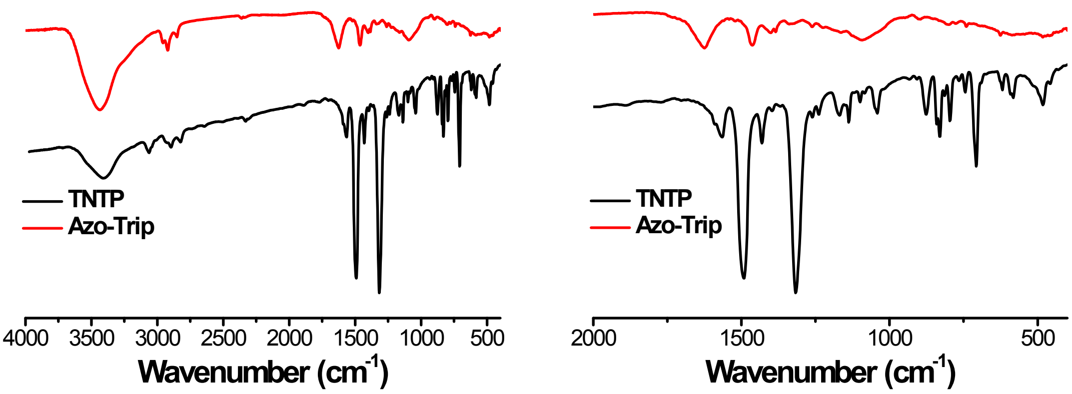

(a) (b)

**Fig. S1.** IR spectra of Azo-Trip and related starting materials TNTP (a) 2000-400 cm$^{-1}$. (b) 2000-400 cm$^{-1}$.

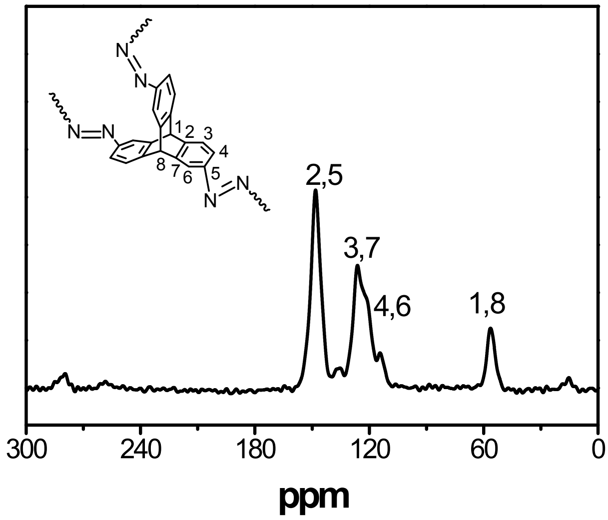

**Fig. S2.** $^{13}$C CP/MAS NMR spectroscopy of the Azo-Trip.

## Section 4. Powder X-Ray Diffraction, SEM image and TGA profiles

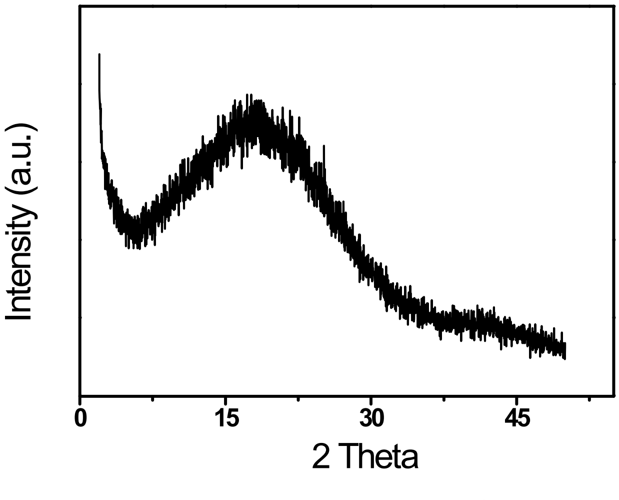

**Fig. S3.** PXRD curve of Azo-Trip.

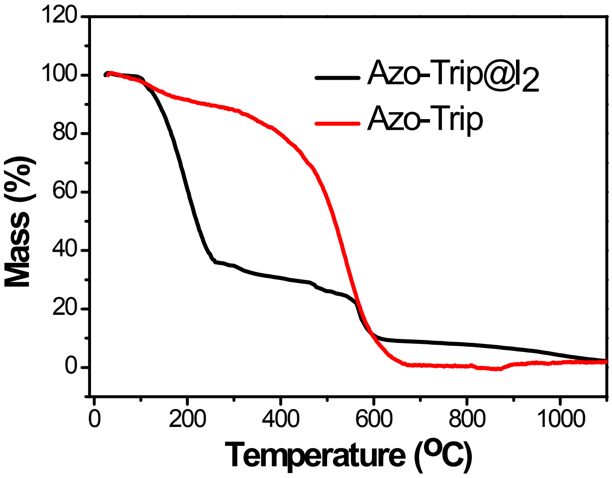

**Fig. S4.** TGA plot of Azo-Trip under $N_2$ condition

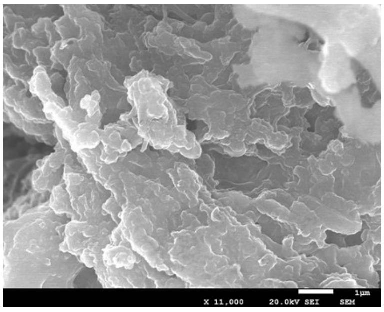

**Fig. S5.** SEM image of Azo-Trip.

## Section 5. Additional gas adsorption data for Azo-Trip

The Langmuir-Freundlich equation is used to fit $CO_2$ and $H_2$ adsorption isotherm and predict the adsorption capacity of the framework at saturation, and Clausius- Clapeyron equation is applied to the calculation of the enthalpies of $CO_2$ and $H_2$ adsorption.

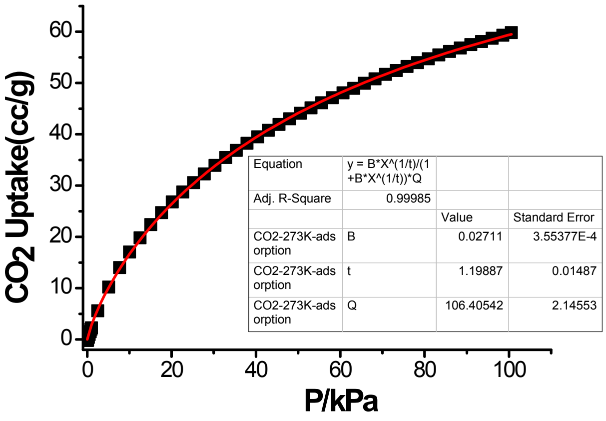

| Equation | y = B*X^(1/t)/(1+B*X^(1/t))*Q | | |
|---|---|---|---|
| Adj. R-Square | 0.99985 | | |
| | | Value | Standard Error |
| CO2-273K-adsorption | B | 0.02711 | 3.55377E-4 |
| CO2-273K-adsorption | t | 1.19887 | 0.01487 |
| CO2-273K-adsorption | Q | 106.40542 | 2.14553 |

**Fig. S6.** $CO_2$ isotherm at 273 K (symbols) and Langmuir-Freundlich equation fits (line) for Azo-Trip.

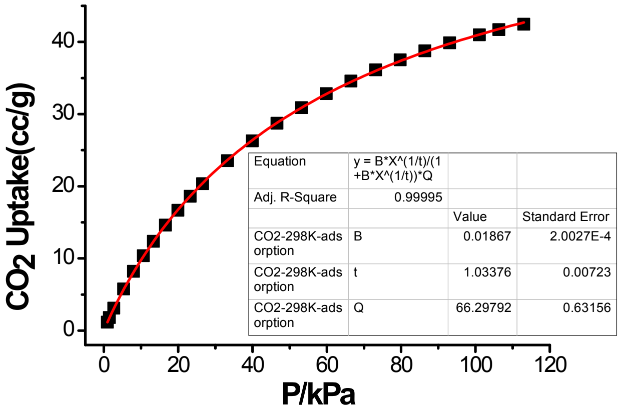

| Equation | y = B*X^(1/t)/(1+B*X^(1/t))*Q | | |
|---|---|---|---|
| Adj. R-Square | 0.99995 | | |
| | | Value | Standard Error |
| CO2-298K-adsorption | B | 0.01867 | 2.0027E-4 |
| CO2-298K-adsorption | t | 1.03376 | 0.00723 |
| CO2-298K-adsorption | Q | 66.29792 | 0.63156 |

**Fig. S7.** $CO_2$ isotherm at 298 K (symbols) and Langmuir-Freundlich equation fits (line) for Azo-Trip.

Henry's law selectivities ($S_H$) were calculated by the ratio of Henry's law constants of $CO_2$ ($H_C$) and $N_2$ ($H_N$).

$$S_H = \frac{H_C}{H_N}$$

The Henry's law constants for $CO_2$ and $N_2$ were obtained by the slope of linear fitting of the initial data (pressure less than 0.1 bar) of the gas adsorption isotherms.

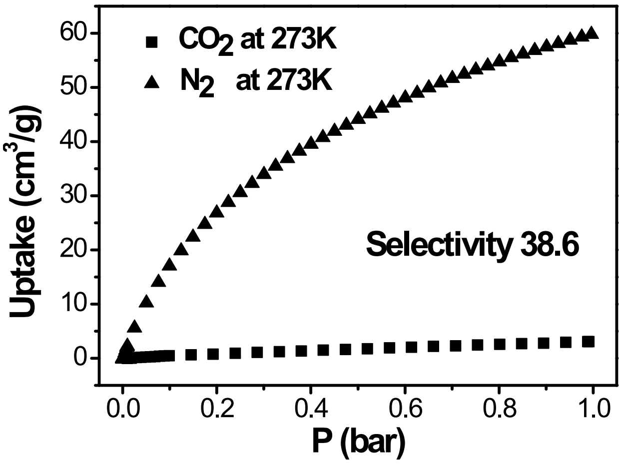

**Fig. S8.** $CO_2$ and $N_2$ adsorption isotherm for Azo-Trip at 273K.

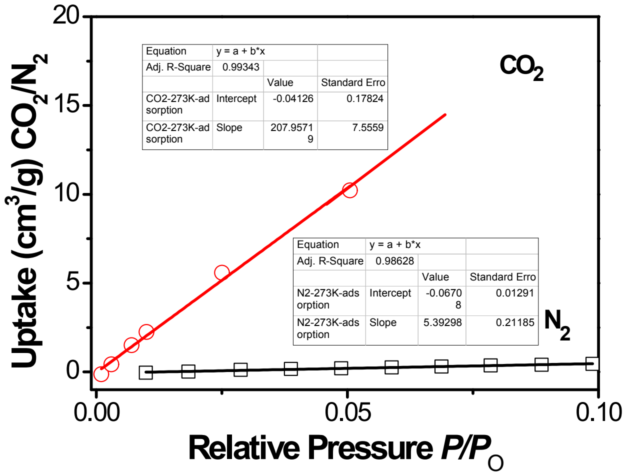

**Fig. S9.** The ideal selectivity of $CO_2$ over $N_2$ was calculated by the Henry's Law.

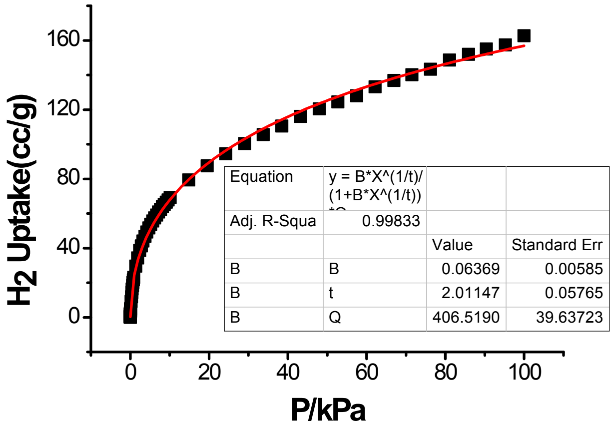

**Fig. S10.** $H_2$ isotherm at 77 K (symbols) and Langmuir-Freundlich equation fits (line) for Azo-Trip.

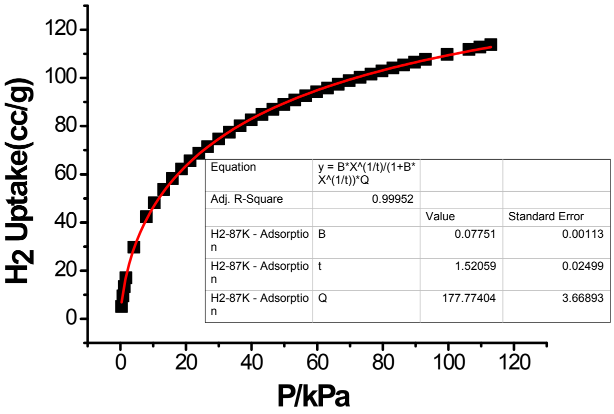

**Fig. S11.** $H_2$ isotherm at 87 K (symbols) and Langmuir-Freundlich equation fits (line) for Azo-Trip.

## Section 6. Calibration plots of standard iodine by UV/vis spectra.

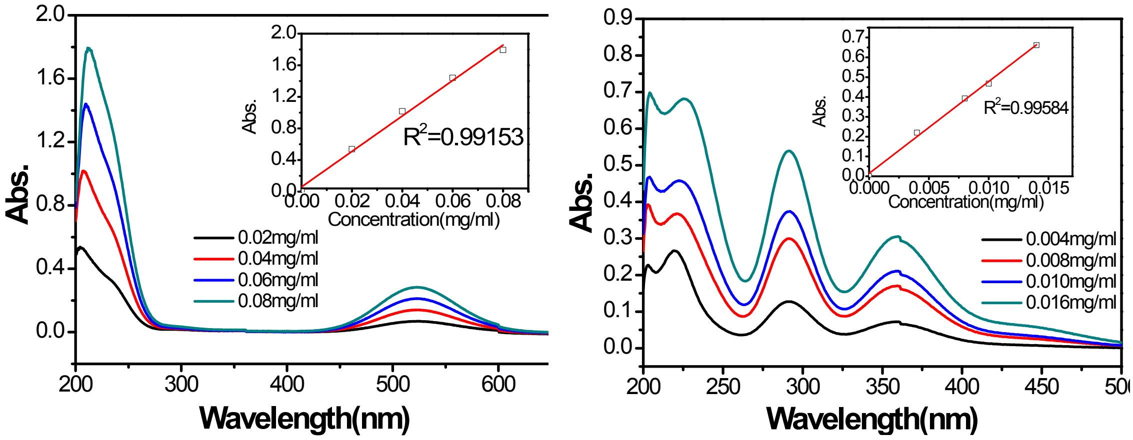

(a) (b)

**Fig. S12.** (a) Calibration plots of standard iodine by UV/vis spectra in cyclohexane solution and (b) ethanol solution, respectively. Inset: the fitting of Abs value *vs* concentration of $I_2$ with the relatively good linearity satisfies Lambert-Beer Law.

## Section 7. Recycable Uptake for Iodine

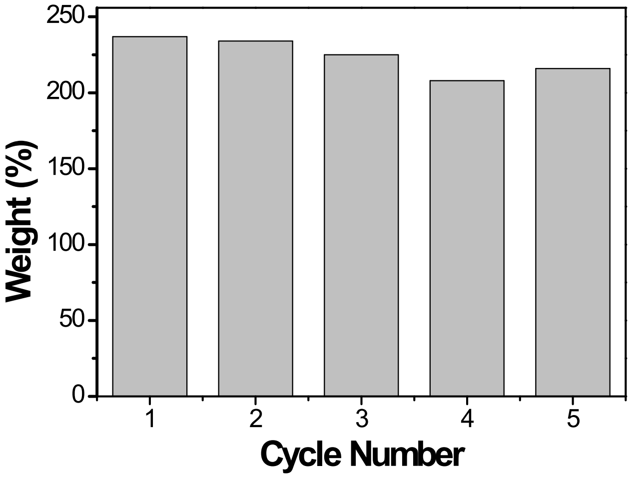

**Fig. S13.** Reusability of Azo-Trip for iodine adsorption by vapor sublimation.

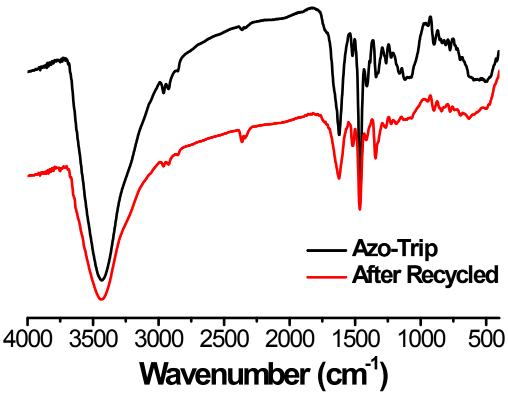

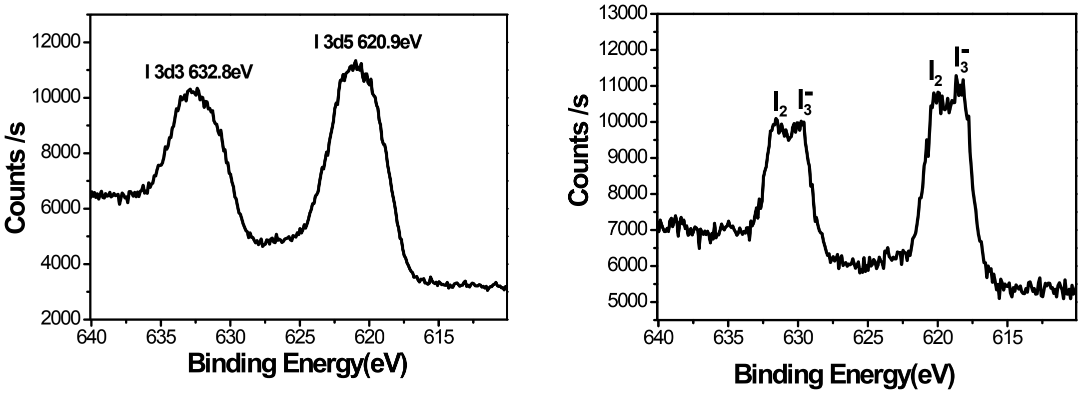

(a) (b)

**Fig. S15.** XPS spectra of (a) Azo-Trip@$I_2$ and (b) recycled five times for Azo-Trip after washed by ethanol.

**Fig. S14.** IR spectra of Azo-Trip and after recycled five times for Azo-Trip.

## Section 8. Sorption Kinetics

### The Pseduo-second-order model

The linear form of pseudo second order kinetic model is expressed by the following equation:

$$\frac{t}{Q_t} = \frac{1}{k_2 Q_e^2} + \frac{t}{Q_e}$$

Where Qt and Qe are the mass percent of iodine absorbed at time $t$ and equilibrium, $k_2$ is the pseudo-second-order rate constant of adsorption process.

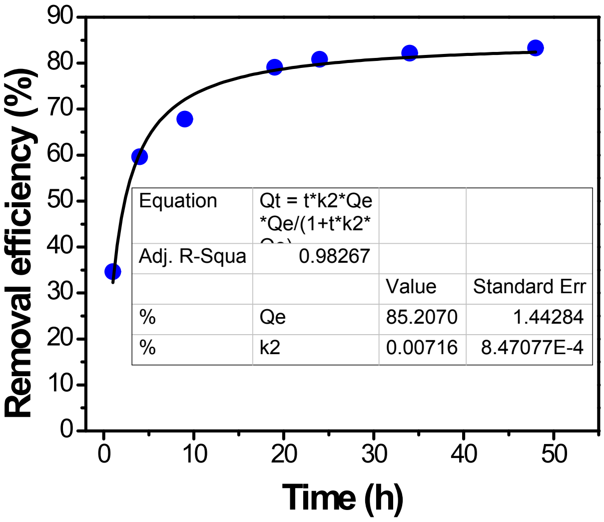

| Equation | Qt = t*k2*Qe *Qe/(1+t*k2* | | |
|---|---|---|---|
| Adj. R-Squa | 0.98267 | | |
| | | Value | Standard Err |
| % | Qe | 85.2070 | 1.44284 |
| % | k2 | 0.00716 | 8.47077E-4 |

**Fig. S16.** Iodine sorption kinetics analyzed by Lagergren pseudo-second-order kinetic models.

## Section 9. Photography of color change

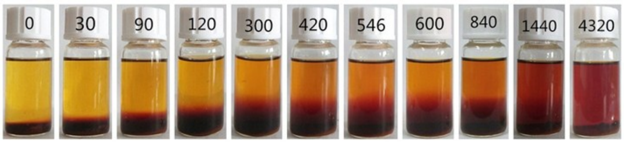

**Fig. S17.** The color change of the ethanol solution (10 ml) of Azo-Trip@$I_2$ (1mg) with time (min).

## Section 10. Release of Iodine

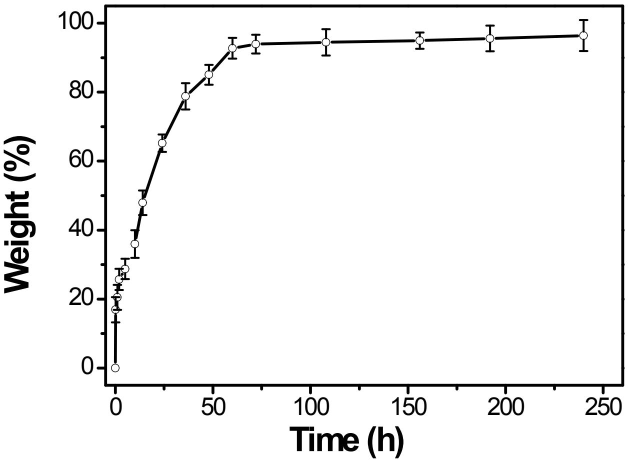

**Fig. S18.** Temporal evolution of the $I_2$-release amount for Azo-Trip@$I_2$.

## REFERENCES

(S1) C. Zhang and C. Chen, *J. Org. Chem.*, 2006, **71**, 6626-6629.